Metallomics

Accepted Manuscript

This article can be cited before page numbers have been issued, to do this please use: I. E. León, P. Díez, S. B. Etcheverry and M. Fuentes, *Metallomics*, 2016, DOI: 10.1039/C6MT00045B.

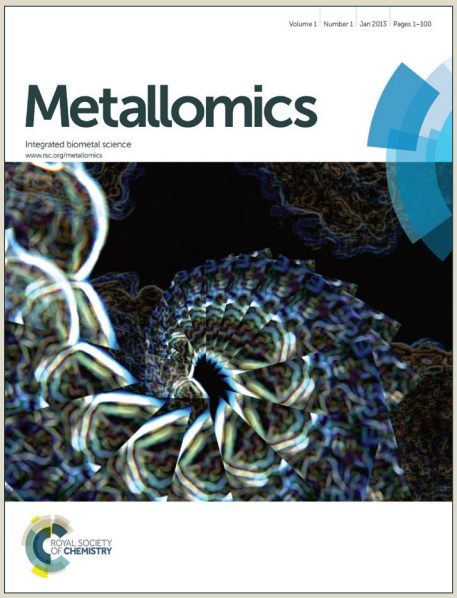

ROYAL SOCIETY OF CHEMISTRY

www.rsc.org/metallomics

View Article Online
DOI: 10.1039/C6MT00045B

Deciphering the effect of an oxovanadium(IV) complex with the flavonoid chrysin (VOChrys) in intracellular cell signalling pathways in osteosarcoma cell line

Ignacio E. León [1,2], Paula Díez [3,4], Susana B. Etcheverry [1,2] * and Manuel Fuentes [3,4] *

[1] Chair of Patologic Biochemistry, Exact School Sciences, National University of La Plata, 47 y 115, 1900 La Plata, Argentina.

[2] Inorganic Chemistry Center (CEQUINOR, CONICET), Exact School Sciences, National University of La Plata, 47 y 115, 1900 La Plata, Argentina.

[3] Cancer Research Center. University of Salamanca-CSIC. IBSAL. Department of Medicine. Servicio General de Citometría-Nucleus. Campus Miguel de Unamuno S/N. 37007 Salamanca. Spain.

[4] Proteomics Unit. Cancer Research Center. IBSAL. University of Salamanca-CSIC. Campus Miguel de Unamuno S/N. 37007 Salamanca. Spain.

*** Corresponding authors:**

Manuel Fuentes, Ph.D. Department of Medicine and General Cytometry Service-Nucleus, Cancer Research Centre (IBMCC/CSIC/USAL/IBSAL). Avda. Universidad de Coimbra S/N, 37007 Salamanca, Spain. Tel.: +34 923294811; Fax: +34 923294743. e-mail: mfuentes@usal.es

Susana B. Etcheverry, PI, Chair of Patologic Biochemistry, Exact School Sciences, National University of La Plata, 47 y 115, 1900 La Plata, Argentina. e-mail: etcheverry@biol.unlp.edu.ar

View Article Online
DOI: 10.1039/C6MT00045B

ABSTRACT

Vanadium complexes were studied during recent years to be considered as a representative of a new class of non-platinum metal antitumor agents in combination to its low toxicity. However, a few challenges are still remaining for the discovery of new molecular targets of these novel metal-based drugs. The study of cell signaling pathways related to vanadium drugs are scarcely reported and so far this information is highly critical for identifying specific targets that play an important role in the antitumor activity of vanadium compounds. This research deals with the alterations in intracellular signaling pathways promoted by an oxovanadium(IV) complex with the flavonoid chrysin $[VO(chrysin)_2EtOH]_2$,(VOChrys) on a human osteosarcoma cell line (MG-63). Herein it is reported for the first time, in order to identify targets of $[VO(chrysin)_2EtOH]_2$, the relative abundance of 224 proteins which are involved in most of the common intracellular pathways. Besides, full-length human recombinant (FAK and AKT1) kinases are produced by *in situ* IVTT system and then we have evaluated the variation of relative tyrosin-phosphorylation levels caused by $[VO(chrysin)_2EtOH]_2$ compound. The results of the differential protein expression levels reveal several proteins altered such as PKB/AKT, PAK, DAPK, Cdk 4, 6 and 7, FADD, AP2, NAK, JNK, among others. Moreover, cell signaling pathway involved in several altered pathways related to PTK2B, FAK, PKC family, suggesting the important role associated with the antitumor activity of $[VO(chrysin)_2EtOH]_2$. Finally, the effect of this compound on *in situ* expressed FAK and AKT1 is validated by determining the phosphorylation level which is decreased in the first one and increased in the second one.

View Article Online
DOI: 10.1039/C6MT00045B

Keywords: Cell Signaling, Vanadium, Osteosarcoma, Functional Proteomics, FAK, anticancer agents.

View Article Online
DOI: 10.1039/C6MT00045B

Significance Statement

Understanding how vanadium-flavonoid complexes perform their role as antitumor agents is key in the metal-based drugs field. While many mechanisms of action for vanadium compounds are known and have been characterized (ROS generation, apoptosis induction, tyrosine phosphatase inhibition, and ERK1 and ERK2 activation, among others), this present project exposes evidences about the role and function of two novel molecular targets (FAK and AKT1) involved in the antitumor effects of vanadium compounds against bone cancer.

View Article Online
DOI: 10.1039/C6MT00045B

Introduction

Metal ions drugs conjugates regulate and participate in a widespread array of vital cellular processes with high specificity and selectivity. The ability of several metal ions conjugates as cancer therapeutic agents have since long been known, with early documented cases dating back to the 16th century [1]. However, a few challenges are still remaining (such as lack of specificity, poor absorption, high cytotoxicity, chemoresistance). In this sense, bioinorganic and medicinal chemistry are exploring different strategies to overcome these problems, which includes targeted delivery of clinical drugs, design, and synthesis of novel metal-based drugs which have different structural features and reactivities[2,3]. As a consequence, a significant number of anticancer metallodrugs have recently emerged, two of the most actives of which are platinum [4] and vanadium [5]. In the case of platinum, cisplatin, carboplatin and oxaliplatin are the most important and successful metal-based drugs in the clinic, in spite of their severe side effects [6]. On the other hand, the pharmacological actions of vanadium convert its compounds into possible therapeutic agents to be used in the treatments of several pathologies such as cancer, among others. In fact, the antitumor effects of vanadium compounds have been widely *in vitro* tested on various different types of malignant cell lines. Metvan [$V^{IV}O(SO_4)(4,7\text{-Mephen})_2$] was identified as one of the most relevant vanadium complex with antitumor activity against different pathological cell lines of human origin such as leukemia cells, multiple myeloma cells and solid tumor cells derived from glioblastoma, breast cancer, ovarian, prostate and testicular cancer patients [7–9]. Other interesting groups of vanadium compounds with antitumor properties is vanadocene derivatives that show promising therapeutic effects toward human cancer cells derived from liver, testicular, among others [10,11].

View Article Online
DOI: 10.1039/C6MT00045B

The role of vanadium in the regulation of intracellular signaling pathways converts it in a potential therapeutically agent to be used in several diseases. Nevertheless, the study of cell signaling pathways targeted by vanadium complexes are scarcely reported in the literature and so far these data for the discovery of new molecular targets in cancer have not been completely examined.

Previously reported results demonstrated that several vanadium-flavonoid compounds caused cyto- and genotoxicity, induced by cell cycle arrest and apoptosis in human osteosarcoma cells [12,13]. In this context, it is a huge interest in deciphering the targets of vanadium compounds on the cell signaling pathways in their antitumor effects.

In the last years, protein microarrays have emerged as a high-throughput approach to provide a suitable tool for the discovery of novel drug targets, cancer biomarkers, and determination of relative protein abundance, among others[14]. Despite the progress in protein microarrays area, and the multiple applications; a few challenges are still remaining in this area, such as protein stability and functionality, among others. Hence, in order to overcome these challenges a complemented method has been developed a novel array technology called NAPPA (Nucleic Acids Programmable Protein Arrays) technology. A new generation of self-assembled protein microarray where cDNAs, encoding human proteins with a tag, are spotted onto chemically modified surfaces. In the NAPPA, full-length proteins are produced *in situ* by using cell-free protein expression systems[15]. The emerging protein is captured by immobilized antibodies specific for the tag encoded at the carboxy-terminus of the amino acid sequence, which ensures the full-length translation of the captured protein. Full-length human recombinant proteins *in situ* expressed have been successfully applied in the study of post-translational modification of proteins, protein-protein interaction, and protein-drug interactions [16].

View Article Online
DOI: 10.1039/C6MT00045B

Here, it is proposed to identify novel targets of vanadium compounds (with potential pharmacological applications) by using both protein array platforms (relative abundance based antibody arrays and in situ protein arrays). This study deals with the effects of intracellular signaling of an oxovanadium(IV) complex with the flavonoid chrysin $[VO(chrysin)_2EtOH]_2$, on a human osteosarcoma cell line (MG-63). We have investigated and report herein for the first time, the action of $[VO(chrysin)_2EtOH]_2$ on the relative abundance protein patterns of 224 proteins involved in most common intracellular signaling pathways.

In addition, full-length human recombinant (FAK and AKT1) kinases are produced *in situ* using rabbit reticulocyte lysate (RRL) *in vitro* protein expression systems and we have explored the protein expression level and the tyrosine phosphorylation sites inhibition induced by $[VO(chrysin)_2EtOH]_2$.

Experimental Section

Materials

Tissue culture materials were purchased from Corning (Princeton, NJ, USA), RPMI 1640 (Sigma Chemical Co. ST. Louis, MO), trypsin and fetal bovine serum (FBS) from Gibco (Gaithersburg, MD, USA), RC DC Protein Assay Kit from Bio-Rad, Protein-G-agarose beads, Cy3 and Cy5 from GE Healthcare, Purefield™ Plasmid Miniprep System from Promega, Antibody anti phosphotyrosine from Millipore, polyclonal anti-GST from GE Healthcare, monoclonal anti-GST from Cell Signaling, anti-mouse-HRP from Jackson ImmunoResearch Laboratories, West Grove, PA Panorama Cell Signalling Kit (Sigma

View Article Online
DOI: 10.1039/C6MT00045B

Chemical Co. ST. Louis, MO). All other chemicals were from Sigma Chemical Co. (ST. Louis, MO). MG-63 cell line was purchased from ATCC.

Methods

Synthesis and Identification of $[VO(chrysin)_2EtOH]_2$

$[VO(chrysin)_2EtOH]_2$ was synthesized according to previously reported results [17]. Briefly, chrysin (0.5 mmol) was mixed with vanadyl acetylacetonate (0.25 mmol) in absolute ethanol and refluxed for ca. 1.30 h (final pH = 5). The hot green suspension was filtered; the solid was washed three times with absolute ethanol and air-dried. Anal. Calc. for $C_{64}H_{48}O_{20}V_2$: C, 62.0; H, 3.9; V, 8.2. Exp.: C, 62.0; H, 4.1; V, 8.1. Yield: 70%.

The identification of the complex was done by FTIR. The main vibrations of the organic moiety were: 1631 s; 1596 s; 1521 vs; 1428 s; 1350 s; 1161 vs. The vibration corresponding to the v(VvO) with a medium intensity was placed at 968 cm^{-1}.

Preparation of $[VO(chrysin)_2EtOH]_2$ Solutions

Fresh stock solutions of the complex were prepared in DMSO at 20 mM and diluted according to the concentrations indicated in the legends of the figures. We used 0.5% as the maximum DMSO concentration in order to avoid toxic effects of this solvent for the cells.

Stability of the Complexes in Solution

To test the stability of $[VO(chrysin)_2EtOH]_2$ under different experimental conditions used in this work, we analyzed the UV–visible spectra of different solutions of the complex. $[VO(chrysin)_2EtOH]_2$ 20 mM solutions in DMSO and RPMI medium with 0.5% of DMSO

View Article Online
DOI: 10.1039/C6MT00045B

(pH= 7.4) were prepared. The electronic spectra were recorded at times ranging from 0 to 6 h. The rate of decomposition of the complex was spectrophotometrically measured.

Cell Culture Conditions

MG-63 cells were grown in RPMI 1640 containing 10 % FBS, 100 U/mL penicillin and 100 µg/mL streptomycin at 37 °C in 5% CO_2 atmosphere. Cells were seeded in a 175 cm^2 flask and when 70-80 % of confluence was reached, cells were subcultured using 4 mL of trypsin per 175 cm^2 flask. For experiments, cells were grown in 75 cm^2 flask for 24 h at 37 °C. Then, the monolayer was incubated with different concentrations (25 and 100 µM) of the complex.

Subcellular Protein Fractionation and Dye-Labeling

Cytoplasmic proteins were isolated by using sub-fractionation protocol. The cells were harvested and washed three times with PBS. Then, it was added three volumes of lysis buffer (5mM HEPES, 10mM $MgCl_2$, 140mM NaCl, 0.1% (v/v) Tween 20 at pH 8.0, 1% (v/v) protease inhibitor mix. Briefly, lysed cells were centrifuged for 15 min at 15000 *g* at 4°C. After that, the supernatant was collected and 10% (w/v) octyl-β-D- glucopyranoside was added followed by sonication (3 times with 3-second bursts). Samples were preserved on ice for 30 min and then centrifuged obtaining the cytoplasmic fraction.

Immediately after IgG depletion (by using protein-G-agarose beads), purified proteins were quantified by Lowry assay following the manufacturer's instructions. Then, cytoplasmic proteins were conjugated with Cy3 or Cy5 at >2 dye/protein ratio following manufacturer's recommendation's.

View Article Online
DOI: 10.1039/C6MT00045B

Panorama Antibody Microarray Assays

Functional Proteomic Analysis was performed by using the Panorama Cell Signaling Kit following the manufacturer's instructions. The antibody microarray consists of 224 human monoclonal antibodies targeting proteins involved in intracellular signaling pathways, spotted in duplicate onto the nitrocellulose-coated slide. Equal amounts of fluorescently labeled proteins of osteosarcoma cells from basal condition (control) and from treatments with vanadium complex (each with a different dye) was incubated with the microarray slide at RT for 1 h on an orbital shaker. For optimal and robust characterization of differences in relative protein abundance in all the tested conditions and according to the manufacturer only the proteins which presented a Cy5/Cy3 ratio Cy5/Cy3 ≥ 2 (up) and a ratio Cy5/Cy3 $\leq$ 0.5 (down) have been taken into consideration for the identification of altered intracellular pathways.

Antibody Microarray Data Analysis

Microarrays were scanned with Scanner GenePix 4000B (Axon, USA) using Cy3 and Cy5 settings. The images were analyzed with GenePix Pro 4.0 software (Axon, USA).

First of all, background correction for each spot was locally made by applying standardized settings of GenePix software. Then, the mean value of the set of negative control spots in each fluorescence channel was subtracted from the individual spot values. Before statistical analysis (MultiExperiment Viewer (MeV) clustering, and Significance Analysis of Microarrays (SAM)), raw intensity data for each slide were normalized by reference (housekeeping) proteins. The fluorescence intensity obtained for each protein in the array was divided by the fluorescence intensity obtained for a highly expressed reference protein.

View Article Online
DOI: 10.1039/C6MT00045B

We performed a Z-score estimation for the housekeeping proteins in the array and selected those with a high value (>2) for the normalization.

In all cases, the mean of the protein replicates was calculated to obtain a single value *per* protein/assay [18].

Functional Annotation of Down/Up-Regulated Expressed Proteins

Altered–expression proteins were selected by computing a relation between each condition (control *vs* vanadium treatment) after applying the normalization strategy describe above. Significance was assigned to proteins whose ratio was greater than or equal to 2.0 or fewer than or equal to 0.5.

Functional annotation of selected proteins was analyzed with GeneCodis tool including gene ontology (GO) annotations and Circos software.

Self-Assembled (NAPPA-ELISA) Protein Arrays

The list of candidate kinases selected for targeted screening was built on the basis of the Panorama Cell Signaling Kit results. The two cDNAs (encoding corresponding full-length human proteins) employed in the NAPPA Elisa are FAK and AKT1.

cDNA Preparation

Escherichia coli bearing a total of 2 sequence-verified full-length human genes in pANT7_cGST were obtained from the Center for Personalized Diagnostics at the Arizona State University and are publicly available (www.dnasu.org). Bacteria were grown for 24 h at 37 °C in 100 mL of Luria−Bertani medium supplemented with ampicillin for cGST clones. The cells were pelleted and their plasmid DNA was purified using Purefield™ Plasmid Miniprep System according to the manufacturer's instruction.

View Article Online
DOI: 10.1039/C6MT00045B

In Situ Protein Expression

The *in vitro* transcription and translation step was performed as previously described by Manzano-Román et al. [19] The transcription/translation lysate mix was added into the tubes. The tubes were incubated for 1.5 h at 30 °C for protein expression and captured by anti-GST polyclonal, respectively.

ELISA Assay

A GST fused to the full-length human FAK and AKT1 were expressed *in vitro* using the rabbit reticulocyte lysates, as previously described [19,20].

The FAK and AKT1 proteins were then applied to an anti-GST-coated 96-well plate. Plates were washed in PBS-0.02 % Tween and blocked with PBS-Tween with 5 % milk, overnight at 4 °C. After washing, the plate was incubated with the 1:1000 (v/v) diluted antimouse-GST and anti mouse-phosphotyrosine antibodies. The presence of specific protein was detected by incubation with the HRP-linked anti mouse secondary antibody (Jackson ImmunoResearch Laboratories, West Grove, PA) diluted 1:1000 (v/v) in assay buffer. Tetramethylbenzidine substrate was then added and the reaction stopped. The 450 nm signals were read and the absorbances were subjected to *t*-test analysis to determine the significance of any variation in antibody levels between samples.

View Article Online
DOI: 10.1039/C6MT00045B

Results and Discussion

Synthesis and Characterization of $[VO(chrysin)_2EtOH]_2$

$[VO(chrysin)_2EtOH]_2$ (Figure 1A) was synthesized as previously described by Naso et al. [17] (see Materials and Methods section). The final product was characterized by FTIR, being the main vibrations fully comparable with the organic moiety, allowing a proper identification. Moreover, from the EPR data, it was assumed that in the proposed complex structure for $[VO(chrysin)_2EtOH]_2$ the axial positions were occupied by the oxygen atom of VO and the other axial position by a solvent molecule. The equatorial positions are occupied by two organic ligand molecules, and in solution, it can be assumed that the main species is VOL_2, taking into account the L/M ratio. On the other hand, it has been described that chrysin ligand form penta-coordinated species with (CO, O^-) or "acetylacetone-like" coordination showing dimer configuration of chrysin complex at physiological pH (see Figure 1B and 1C) , as it was previously reported by Sanna et al. [21] . These acetylacetone-like species display low interaction with the proteins and different biomolecules present in peripheral blood, keeping their structure because of the good stability under physiological conditions [22].

Stability Assays

Since DMSO has been used as a co-solvent in a biological system, we explored the stability of the $[VO(chrysin)_2EtOH]_2$ complex in DMSO and RPMI solution (pH=7.4) using UV- vis spectroscopy. In the electronic absorption spectrum of $[VO(chrysin)_2EtOH]_2$ (0.02 M in DMSO solution) two d–d transitions were observed at 576 (ε=16 M^{-1} cm^{-1}), and 794 nm (ε=32 M^{-1} cm^{-1}) according to previously reported by Naso [17]. Monitoring this solution

View Article Online
DOI: 10.1039/C6MT00045B

along the time (0.25, 0.5, 1, 2, 3 and 6 h), no changes were observed in the UV-vis signals, and the integrity of the complex in DMSO was intact within the time-frame of the biological experiments (see **Supporting Information S1A**). Besides, in the electronic absorption spectrum of $[VO(chrysin)_2EtOH]_2$ (0.0001 M, in RPMI solution), as it can be seen the characteristic band II of flavones in the 250–285-nm range representing A ring (benzoyl system, $\pi = \pi^*$) absorption. Checking this solution along the time (0.25, 0.5, 1, 2, 3 and 6 h), no changes were observed in the UV-vis signal, and the integrity of the compound in RPMI medium solution (pH=7.4) was not modified within the tested time (see **Supporting Information S1B**).

These results and EPR spectroscopy results previously reported by Naso et al.[17] suggesting that the compound does not undergo oxidation and is stable over time.

Cytotoxic Activity of $[VO(chrysin)_2EtOH]_2$ in Human Osteosarcoma MG-63 Cells

$[VO(chrysin)_2EtOH]_2$ caused a concentration-dependent inhibition of cell viability in human osteosarcoma MG-63 cells. The anti-proliferative action of the complex is much stronger as a consequence of a cooperative/ synergy effect of the free flavonoid and the vanadyl cation; demonstrating the improvement of the antitumor action through the complexation of the chrysin with vanadyl(IV). This is also evident from the IC_{50} values in MG-63 cells: $[VO(chrysin)_2EtOH]_2$ ca.16 μM while for chrysin and $VO^{(+2)}$ the IC_{50} are >100 μM [12]. The complex disrupted the GSH levels and the mitochondria membrane potential (MMP). Besides, $[VO(chrysin)_2EtOH]_2$ increased ROS production, and levels of caspase 3 and DNA fragmentation on MG-63 cells after 24 h of treatment [12]. Moreover, $[VO(chrysin)_2EtOH]_2$ did not show antiproliferative effects on MG-63 cells at 25 and 100 μM after 3 h of incubation but the compound impaired cell viability (25 % of cytotoxicity)

View Article Online
DOI: 10.1039/C6MT00045B

at 100 μM after 6 h of treatment suggesting a key role of concentration and incubation time as laying events for the deleterious effects of this vanadium complex. In accordance with these results, after 3 h of treatment, $[VO(chrysin)_2EtOH]_2$ did not cause any change in the externalization of PS either at 25 or at 100 μM. Nevertheless, after 6 h of incubation, these concentrations of the complex produced ca. 20% of apoptotic cells (Annexin V+) with statistically significant differences in the basal condition [12].

On the other hand, the results indicate that $[VO(chrysin)_2EtOH]_2$ had greater antitumor actions in human osteosarcoma cells than in non-transformed osteoblasts [12]. Moreover, no deleterious effects were detected in peripheral mononuclear blood cells (PMBC) used as control cells[12].

As a whole, these results demonstrate that $[VO(chrysin)_2EtOH]_2$ is a potentially good candidate for further evaluation of its molecular targets since it was less toxic to the normal phenotype cells (MC3T3-E1 and PMBC) and was highly deleterious for the human osteosarcoma cells.

Deciphering Simultaneously Altered Cell Signaling Pathways by $[VO(chrysin)_2EtOH]_2$ Treatment in Osteosarcoma MG-63 Cells

Bearing in mind a previously reported compound characterization [12], in order to identify relative differences in protein profiles a time and concentration course treatment in MG-63 cells with vanadium-chrysin complex were performed with abundance-based protein arrays as described in the Materials and Methods section. In summary, the experimental workflow is briefly described in Figure 2. According to well-characterized reported info about $[VO(chrysin)_2EtOH]_2$, several comparison assays were performed with soluble proteins (i.e. cytoplasmatic, nuclear, among others), from basal conditions (called controls) and different

View Article Online
DOI: 10.1039/C6MT00045B

treatment conditions with $[VO(chrysin)_2EtOH]_2$ (25 μM 3 h, 25 μM 6 h and 100 μM 6 h). Representative images of these experiments are displayed in Figure 3. This experimental design allows to decipher altered cell signaling pathways by the effect of $[VO(chrysin)_2EtOH]_2$ from studying global differential protein expression profiles, and the potential correlation with the antitumor effect of this compound in solid tumors (as a model we used human osteosarcoma cells).

Table I. Effects of $[VO(chrysin)_2EtOH]_2$ in relative protein abundance.

Condition	Concentration (μM)	Time (h)	Up-regulated proteins	Down-regulated proteins
1	25	3	22	2
2	25	6	27	8
3	100	6	82	9

Table I shows that after 3h and 25 μM $[VO(chrysin)_2EtOH]_2$ treatment (condition 1), twenty-two up-regulated proteins and only two down-regulated proteins were detected (see Supporting information S2) while for condition 2 $[VO(chrysin)_2EtOH]_2$ up-regulated twenty-seven and down-regulated eight proteins (see Supporting information S3). In condition 3, the complex up-regulated eighty-two proteins and it caused down-regulation of nine proteins (see Supporting Information S4); in contrast with, condition 3 presents major differences in the number of down- and up-regulated proteins than for the other conditions.

Overall, these results demonstrate the presence of significant differences in protein expression patterns as a consequence of the expected targeted effect of this drug in several intracellular signaling pathways. The main proteins identified within differential expression profiles are grouped and discuss below in canonical signaling pathways: 1.-Apoptosis, 2.-Cell cycle, 3.-Signalling transduction.

View Article Online
DOI: 10.1039/C6MT00045B

Effect of $[VO(chrysin)_2EtOH]_2$ Concentration on Alteration of Cell Signaling Pathways

Figure 4 shows a summary of altered relative protein abundance detected in each treatment with $[VO(chrysin)_2EtOH]_2$. As it can be seen in the Figure 4A (6 h, at 25 and 100 μM) the compound concentration plays a role in the increment of relative levels of Bcl-x, caspase 6, 7 and 10. Besides, for condition 2, the level of phosphatidylserine receptor (early apoptosis biomarker) is higher than for condition 3 according to previously reported results [12]. In addition, this compound shows an effect in up-regulation of caspase 4, 5, 11 and DAP-kinase at 100 μM (see Supporting information S4) suggesting a higher level of late cell death proteins, in concordance with previously published results [12]. Moreover, both treatments (condition 2 and 3) seem to induce the up-regulation of c-myc, Ap-1/cJun, HADC4 and PCAF. At 100 μM of $[VO(chrysin)_2EtOH]_2$, the relative abundance of Ap-1/cJun is higher than at 25 μM, suggesting the key role of these transcription factors in cell cycle progress and apoptosis. On the other hand, samples treated with 100 μM of $[VO(chrysin)_2EtOH]_2$ presented low levels of Cdc6 and Cyclin D1, while Cyclin A and D3, Cdc25 and CDK4, 6 and 7 were up-regulated. These results confirm an increment in cell cycle activity in direct relation with the function of the concentration of $[VO(chrysin)_2EtOH]_2$, which have been previously reported in several studies [12].

Seven up-regulated proteins were in common identified between condition 2 and 3 (Figure 4A). In both cases, there was an enrichment in FAK (Tyr^{577}), MAPK8, MAPK1/3, PKC a, PKC b, PKC g and PTK2B. In this sense, MAPK cascade is one of the major signaling pathways apparently involved in global biological effects of vanadium. Srivastava and co-workers reported that the stimulation of the ras-ERK pathway by vanadyl sulfate is dependent on PI3-K activation and it is suggested that the stimulation of these cascade

View Article Online
DOI: 10.1039/C6MT00045B

plays a significant role in mediating the insulin-mimetic effects of inorganic vanadium salts[23]. It has been shown that vanadium salts activate MAPK and two ribosomal protein kinases[24,25].

Moreover, for condition 3, several cytoskeleton-related proteins (cytokeratin family, PAK kinase…) shown up-regulated. In the same way, Nitric Oxide Synthase proteins (iNOS, bNOS, eNOS), phospholipase A2 and AKT1, are also up-regulated. Many scientific reports showed the interaction between vanadium compound with anti-diabetic actions and AKT cell signaling pathway [26,27].

Among similar results as previously reported, the results obtained from these assays depicted an increment of the relative abundance of NF-κB(NFKB1), a crucial nuclear factor that increases survival defecting cell death. Also, a high relative abundance level of JUN proteins was detected, which is considered an important protein in the proliferation and survival of osteosarcoma cells [28]. In the same way, relative levels of PKC were up-regulated, which it could be linked with restoring the proteasome activity and abrogated osteosarcoma cellular differentiation [29].

Other important findings are related to RAF1 which appeared down-regulated. This could lead to the inactivation of the cell cycle through MEK/ERK signaling. However, the significant increase of JNK may act as a counter balance to the negative effect of RAF1.

In addition, MDM2, a principal negative regulator of p53, was decreased while CDKN2A an important stabilizer of p53 was up-regulated under condition 3 of incubation. With this information, it is possible to infer that $[VO(chrysin)_2EtOH]_2$ exert a positive feedback for p53 to mediate the degradation and stabilization of p53. In this way, p53 levels suppress cell proliferation and enhances metastasis and angiogenesis of osteosarcoma, as previously

View Article Online
DOI: 10.1039/C6MT00045B

described by Song et al [30]. Therefore, the down-regulated and up-regulated effects of $[VO(chrysin)_2EtOH]_2$ on MDM2 and CDKN2A could be considered as a novel antitumor therapeutic strategy that exploits the pro-apoptotic effects of p53 against human osteosarcoma.

On the other side, the relative abundance level of Grb2 is down-regulated by effects of $[VO(chrysin)_2EtOH]_2$. This protein is widely expressed and is essential for multiple cellular functions; then the inhibition of Grb2 action blocks transformation and proliferation of several cancer cell types [31]. Besides, Grb2 is an adapter protein that provides a critical link between cell surface growth factor receptors and the Ras signaling pathway. This functional profile makes Grb2 a high priority target for antitumor drug development. These results might be considered as first evidence that links the antitumor vanadium properties with the Grb2 effects.

For Focal adhesion kinase (FAK), the results showed that $[VO(chrysin)_2EtOH]_2$ up-regulated the site of phosphorylation Tyr^{577} but down-regulated Tyr^{397} (see Supporting Information S4). The Tyr^{397} site of tyrosine phosphorylation is the most active and common site in the autocatalytic function of FAK [32]. Therefore, these results suggest that $[VO(chrysin)_2EtOH]_2$ inhibited selectively the autophosphorylation activity of FAK kinase affecting directly the Tyr^{397} site.

FAK also known as protein kinase 2 (PTK2) is a protein tyrosine kinase that regulates, motility, cellular adhesion, proliferation and survival in different types of cells. Interestingly, FAK is well-characterized as over-expressed and activated in several advanced-stage solid cancers and it promotes tumor progression and metastasis [33]. Consequently, FAK has become a potential prognostic marker and antitumor molecular

View Article Online
DOI: 10.1039/C6MT00045B

target [34]. Moreover, research studies showed that FAK plays a key role in integrin signaling. Once activated by integrin and non-integrin stimuli, it binds and activates different molecules, like Grb2, thus promoting signaling transduction [35]. Our results showed that $[VO(chrysin)_2EtOH]_2$ down-regulated Grb2 and, in consequence, its effects could inactivate the cell signaling pathway induced by FAK.

In addition, FAK and EGFR also induced cooperative signals that suppressed apoptosis and enhanced cell survival in breast cancer cells through activation of the ERK and AKT pathways [36].

Effect of Incubation Time of $[VO(chrysin)_2EtOH]_2$ on Altered Cell Signaling Pathways

Figure 4B shows the effects of the time course (3 and 6 h) in the cell signaling pathway altered by 25 μM of $[VO(chrysin)_2EtOH]_2$. As it can be seen that the levels of caspase 7, DDIT3 and phosphatidylserine receptor were higher for condition 2 in comparison with condition 1. These proteins have an important role in the apoptosis induction demonstrating the importance of the time exposure with the drug in the cell death induction [12].

In addition, the data obtained of Figure 4B revealed the up-regulation of FAK, PTK2B and PKC family members. The level of PKC b and PKC g is higher for condition 2 than condition 1, suggesting the importance of these kinases in the antitumor activity of $[VO(chrysin)_2EtOH]_2$. In this order, Mehdi and co-workers established that PKC protein is required to stimulate PKB/AKT phosphorylation in response to anti-diabetic actions of Vanadium(IV) oxo-bis(maltolate) (BMOV) in HepG2 cells [37].

View Article Online
DOI: 10.1039/C6MT00045B

In order to get deeper insights into the biological context, all the up/down differentially expressed proteins in different treatments were subjected to functional characterization using the bioinformatics software DAVID 6.7 (Supporting Information S5-S9).

Identification of Potential Targets with Differential Expression Profiles

We set out to characterize the potential molecular targets and the related pathways involved in the antitumor effects of $[VO(chrysin)_2EtOH]_2$ against human osteosarcoma cells. To perform pathway analysis, the down- and up-regulated proteins identified in each group of treatment have been included in the analysis. In Figure 5, it is represented the different pathway altered proteins detected in the three groups of study (condition 1, 2 and 3). In the analysis of three treatments, most identified proteins were selected (Figure 5). The greatest differences appeared in up-regulation. Samples treated 6 h with 100 μM of $[VO(chrysin)_2EtOH]_2$ (condition 3) exhibited higher levels of PKB/AKT, PAK, DAPK, Cdk 4, 6 and 7, FADD, AP2, NAK, JNK, among others. On the other hand, as it can be seen that PKC family, FAK, and PTK2B were in common in all the treatments suggesting the important role of these proteins associated with the anticancer activity of $[VO(chrysin)_2EtOH]_2$.

In addition, Figure 6 shows the role of these proteins in cancer cell signaling pathways confirming the complexity interaction network of the different kinases involved in antitumor actions of $[VO(chrysin)_2EtOH]_2$. As it can be seen in Figure 6A, PKC and FAK proteins activate PI3K and PKB/AKT which increases of genes transcription levels involved to evading apoptosis, proliferation, and sustained angiogenesis. Besides, Cdk 4 and 6 activate proliferation genes while FADD interacts with caspase-8 and trigger the

View Article Online
DOI: 10.1039/C6MT00045B

apoptosis events. Figure 6B shows the important role of PKC and FAK in focal adhesion signaling pathways. In this order, PKC activated FAK and this protein regulates the activity of PAK. These kinases control the regulation of actin cytoskeleton through activation of the actin polymerization and actin filament turnover.

Functional Validation Assay by IVTT *in situ* Expression of Targeted $[VO(chrysin)_2EtOH]_2$ Kinases

The effect of $[VO(chrysin)_2EtOH]_2$ onto kinases has been validated by functional screening using IVTT recombinant human kinases assays.

Human full-length recombinant AKT1 and FAK kinases (GST-tagged in COOH terminus) were expressed by using cell-free protein IVTT expression system. Hence, AKT1 kinase was selected because of the increment of activity by vanadium compound; however, in the case of FAK, it was selected because its promising therapeutic applications but the effect of $[VO(chrysin)_2EtOH]_2$ is still not fully understood. In both cases, the full-length IVTT expressed protein was detected by GST antibody. The results show that the presence of $[VO(chrysin)_2EtOH]_2$ does not affect the IVTT protein expression.

As it is depicted in Figure 7, $[VO(chrysin)_2EtOH]_2$ compound decreased the FAK-GST relative protein expression level after the treatment with 50 and 100 μM, generating a decrease in translation efficiency of 40 and 95%, respectively (*$p<0.01$). Moreover, the complex only caused a decreased in the AKT1-GST protein expression efficiency at 100 μM whilst at 25 and 50 μM it was not observed any inhibitory effect. In order to study the pattern of tyrosine phosphorylation sites inducing by $[VO(chrysin)_2EtOH]_2$ in both kinases, we evaluated the phospho-tyrosine/GST signal ratio.

View Article Online
DOI: 10.1039/C6MT00045B

Table II shows the effects of $[VO(chrysin)_2EtOH]_2$ on tyrosine phosphorylation for FAK and AKT1 kinases.

Table II. Effects of $[VO(chrysin)_2EtOH]_2$ on tyrosine phosphorylation residues of FAK and AKT1

Ratio Tyr/GST	Control	25 µM	100 µM
FAK	0.54	0.38*	N.D.
AKT1	0.54	0.85*	2.09*

*p<0.01. N.D.: No detectable

The results showed that $[VO(chrysin)_2EtOH]_2$ reduced Tyr/GST ratio suggesting that the complex diminished the level of tyrosine phosphorylation in FAK kinase. These results correlate with the data obtained in the antibody array study, in which we could establish that $[VO(chrysin)_2EtOH]_2$ inhibited selectively the autophosphorylation activity (Tyr^{397}) of FAK kinase. In this way, one of the most attractive sites on the FAK scaffold is the Tyr^{397} autophosphorylation site, due to the unique biology of its interaction with Src and related SH-2 proteins [38]. In fact, this domain provides a new target to inhibit FAK and Src and offers advantages for kinase enzymatic inhibitors that target the ATP-binding site. [39]

Several scientific reports show the discovery of FAK small molecules inhibitors, that effectively decrease Tyr^{397} auto-phosphorylation, preventing cell movement, but do not necessarily induce cell apoptosis in adherent culture conditions [40,41].

On the other hand, $[VO(chrysin)_2EtOH]_2$ increased the Tyr/GST ratio of AKT1 at 25 and 100 µM, respectively. At higher concentration, the complex increases in four-fold the

View Article Online
DOI: 10.1039/C6MT00045B

Tyr/GST ratio, demonstrating the importance of the phosphorylation and activation of AKT pathway in the antitumor vanadium effects.

Several research reports showed that vanadium compounds are potent activators of AKT pathway and protein tyrosine phosphorylation [42,43] (see Supporting Information S10).

Our results show that $[VO(chrysin)_2EtOH]_2$ inhibits selectively the autophosphorylation site (Tyr^{397}) of FAK kinase as well as the efficiency of the translation of this protein. Through these effects, the complex probably diminishes the cell signaling activation by FAK. In this way, $[VO(chrysin)_2EtOH]_2$ affects the normal activity of Grb2 and AKT1 proteins.

Conclusion

New oxovanadium compounds with potential anticancer activity currently require more intensive basic and applied research since this knowledge obtained from in vitro studies may allow vanadium drugs to enter the preclinical in vivo phase. On these bases, we have thoroughly investigated novel targets of oxovanadium(IV)-chrysin complex (with potential antitumor applications) by using protein array platforms (antibody arrays and in situ protein arrays). This study deals with the effects of intracellular signaling of $[VO(chrysin)_2EtOH]_2$ on a human osteosarcoma cell line (MG-63). We have investigated and report herein for the first time, the effects of $[VO(chrysin)_2EtOH]_2$ in intracellular signaling on a human osteosarcoma cell line (MG-63). Besides, we have studied the protein expression level and the tyrosine phosphorylation sites inhibition induced by $[VO(chrysin)_2EtOH]_2$.

The results showed that $[VO(chrysin)_2EtOH]_2$ up-regulated eighty-two proteins and it caused down-regulation of nine proteins such us PKB/AKT, PAK, DAPK, Cdk 4, 6 and 7,

View Article Online
DOI: 10.1039/C6MT00045B

FADD, AP2, NAK, JNK, among others. Besides, the PKC family, FAK, and PTK2B were in common in all the treatments suggesting the important role of these proteins associated with the anticancer activity of $[VO(chrysin)_2EtOH]_2$.

On the other hand, $[VO(chrysin)_2EtOH]_2$ reduced Tyr/GST ratio of FAK but increased the Tyr/GST ratio of AKT1. These results, demonstrating the importance of inactivation of FAK and the phosphorylation and activation of AKT pathway in the antitumor vanadium effects.

Taken together, these results indicate that $[VO(chrysin)_2EtOH]_2$ is an interesting candidate for potential antitumor uses, and provide new insight into the development of vanadium compounds as potential anticancer agents.

Acknowledgments

This work was partly supported by UNLP (11X/690), CONICET (PIP 1125), and ANPCyT (PICT 2008-2218) from Argentina. S.B.E. is a member of the Carrera del Investigador, CONICET, Argentina. I.E.L. has a fellowship from CONICET, Argentina, and a travel grant from National University of La Plata, Argentina. We also gratefully acknowledge financial support from the Carlos III Health Institute of Spain (ISCIII, FIS PI14/01538, and FIS PI12/00624), Fondos FEDER (EU), Junta Castilla-León BIO/SA07/15 and Fundacion Solorzano (FS-23-2015). The Proteomics Unit belongs to ProteoRed, PRB2-ISCIII, supported by grant PT13/0001 (ISCIII-Fondos FEDER). P.D. is supported by a JCYL-EDU/346/2013 Ph.D. scholarship.

View Article Online
DOI: 10.1039/C6MT00045B

Figure Legends

Figure 1. Vanadium complex structure. Chemical proposed structure of oxovanadium(IV)-chrysin complex (A), monomeric configuration of oxovanadium(IV)-chrysin complex under acid condition (B), dimeric configuration of oxovanadium(IV)-chrysin complex at physiological pH (C).

Figure 2. Experimental workflow Global view of the experimental workflow including sample preparation, protein isolation, staining and data analysis).

Figure 3. Representative images of antibody microarrays experiments. They were obtained with scanner GenePix 4000B and processed with GenePix Pro 4.0 software. Scanner settings were identical within microarrays. A) The image shows the upper section of the array (treatment 6 h 100 μM $[VO(chrysin)_2EtOH]_2$). The right image corresponds to a zoom of one block (HAT 1, HDAC 1, 2 and 4 section) in which is highlighted the different color expression between spots depending on the probed samples. B) The left image shows the lower section of the-the array (treatment 6 h 100 μM $[VO(chrysin)_2EtOH]_2$). The right image is a zoom of the selected block (PKB/AKT section).

Figure 4. Main altered proteins detected in each group of treatment. A) Comparison of the Values of ratio Cy5/Cy3 between treatment at 25 and 100 μM of $[VO(chrysin)_2EtOH]_2$ after 6 h of incubation B) Comparison of the Values of ratio Cy5/Cy3 between treatments after 3 and 6 h with 25 μM of $[VO(chrysin)_2EtOH]_2$.

Figure 5. Circos representation. The outer circos's data track shows the differential protein pathways in each group of study. The PKC, FAK, and PTK2B were in common in

View Article Online
DOI: 10.1039/C6MT00045B

all the treatments (colored green, violet and red, respectively). T1 (25 μM 3 h), T2 (25 μM 6 h) and T3 (100 μM 6 h).

Figure 6. Cancer Cell signaling pathways induced by $[VO(chrysin)_2EtOH]_2$. The cell signaling pathway graphic shows the role of different protein down/up-regulated by $[VO(chrysin)_2EtOH]_2$ in cancer pathways **(a)** and focal adhesion **(b)**. The PKC and FAK proteins that were in common in all the treatments (colored yellow). Cdk4/6, FADD, AKT, DAPK, JNK proteins that up-regulated after 6 h with 100 μM of $[VO(chrysin)_2EtOH]_2$ (colored green).

Figure 7. FAK and AKT1 protein expression. A) FAK-GST expression after treatments with 0, 25, 50 and 100 μM of $[VO(chrysin)_2EtOH]_2$ during 180 min. B) AKT1-GST expression after treatments with 0, 25, 50 and 100 μM of $[VO(chrysin)_2EtOH]_2$ during 180 min. (*$p<0.01$) statistical differences between the basal condition and each treatment.

View Article Online
DOI: 10.1039/C6MT00045B

5. References

1 M. Frezza, S. Hindo, D. Chen, A. Davenport, S. Schmitt, D. Tomco and Q. P. Dou, *Curr. Pharm. Des.*, 2010, **16**, 1813–25.

2 J. S. Butler and P. J. Sadler, *Curr. Opin. Chem. Biol.*, 2013, **17**, 175–88.

3 N. P. E. Barry and P. J. Sadler, *Chem. Commun. (Camb).*, 2013, **49**, 5106–31.

4 A. G. Quiroga, *J. Inorg. Biochem.*, 2012, **114**, 106–12.

5 B. Desoize, *Anticancer Res.*, 2004, **24**, 1529–1544.

6 L. Kelland, *Nat. Rev. Cancer*, 2007, **7**, 573–84.

7 Y. Dong, R. K. Narla, E. Sudbeck and F. M. Uckun, *J. Inorg. Biochem.*, 2000, **78**, 321–30.

8 R. K. Narla, Y. Dong, D. Klis and F. M. Uckun, *Clin. Cancer Res.*, 2001, **7**, 1094–101.

9 A. M. Evangelou, *Crit. Rev. Oncol. Hematol.*, 2002, **42**, 249–65.

10 P. Ghosh, O. J. D'Cruz, R. K. Narla and F. M. Uckun, *Clin. Cancer Res.*, 2000, **6**, 1536–45.

11 J. C. Pessoa, S. Etcheverry and D. Gambino, *Coord. Chem. Rev.*, 2014.

12 I. E. Leon, a L. Di Virgilio, V. Porro, C. I. Muglia, L. G. Naso, P. a M. Williams, M. Bollati-Fogolin and S. B. Etcheverry, *Dalton Trans.*, 2013, **42**, 11868–80.

13 I. E. Leon, V. Porro, a. L. Di Virgilio, L. G. Naso, P. a M. Williams, M. Bollati-Fogolín and S. B. Etcheverry, *J. Biol. Inorg. Chem.*, 2014, **19**, 59–74.

14 E. Orenes-Piñero, R. Barderas, D. Rico, J. I. Casal, D. Gonzalez-Pisano, J. Navajo, F. Algaba, J. M. Piulats and M. Sanchez-Carbayo, *J. Proteome Res.*, 2010, **9**, 164–73.

15 N. Ramachandran, J. V Raphael, E. Hainsworth, G. Demirkan, M. G. Fuentes, A. Rolfs, Y. Hu and J. LaBaer, *Nat. Methods*, 2008, **5**, 535–8.

16 J. Huang, H. Zhu, S. J. Haggarty, D. R. Spring, H. Hwang, F. Jin, M. Snyder and S. L. Schreiber, *Proc. Natl. Acad. Sci. U. S. A.*, 2004, **101**, 16594–9.

View Article Online
DOI: 10.1039/C6MT00045B

17 L. Naso, E. G. Ferrer, L. Lezama, T. Rojo, S. B. Etcheverry and P. Williams, *J. Biol. Inorg. Chem.*, 2010, **15**, 889–902.

18 P. Díez, N. Dasilva, M. González-González, S. Matarraz, J. Casado-Vela, A. Orfao and M. Fuentes, *Microarrays*, 2012, **1**, 64–83.

19 R. Manzano-Román, V. Díaz-Martín, M. González-González, S. Matarraz, A. F. Álvarez-Prado, J. LaBaer, A. Orfao, R. Pérez-Sánchez and M. Fuentes, *J. Proteome Res.*, 2012, **11**, 5972–82.

20 F. Henjes, L. Lourido, C. Ruiz-Romero, J. Fernández-Tajes, J. M. Schwenk, M. Gonzalez-Gonzalez, F. J. Blanco, P. Nilsson and M. Fuentes, *J. Proteome Res.*, 2014, **13**, 5218–29.

21 D. Sanna, V. Ugone, G. Lubinu, G. Micera and E. Garribba, *J. Inorg. Biochem.*, 2014, **140**, 173–184.

22 D. Sanna, G. Micera and E. Garribba, *Inorg. Chem.*, 2010, **49**, 174–87.

23 S. K. Pandey, J. F. Théberge, M. Bernier and A. K. Srivastava, *Biochemistry*, 1999, **38**, 14667–75.

24 F. D'Onofrio, M. Q. Le, J. L. Chiasson and A. K. Srivastava, *FEBS Lett.*, 1994, **340**, 269–75.

25 Y. Shechter, J. Li, J. Meyerovitch, D. Gefel, R. Bruck, G. Elberg, D. S. Miller and A. Shisheva, *Mol. Cell. Biochem.*, **153**, 39–47.

26 J.-C. Liu, Y. Yu, G. Wang, K. Wang and X.-G. Yang, *Metallomics*, 2013, **5**, 813–20.

27 M. S. Bhuiyan and K. Fukunaga, *J. Pharmacol. Sci.*, 2009, **110**, 1–13.

28 C. R. Dass, L. M. Khachigian and P. F. M. Choong, *Mol. Cancer Res.*, 2008, **6**, 1289–92.

29 M. Fujita, S. Sugama, M. Nakai, T. Takenouchi, J. Wei, T. Urano, S. Inoue and M. Hashimoto, *J. Biol. Chem.*, 2007, **282**, 5736–48.

30 R. Song, K. Tian, W. Wang and L. Wang, *Int. J. Surg.*, 2015, **20**, 80–7.

31 A. Giubellino, T. R. Burke and D. P. Bottaro, *Expert Opin. Ther. Targets*, 2008, **12**, 1021–33.

32 E. Ciccimaro, J. Hevko and I. A. Blair, *Rapid Commun. Mass Spectrom.*, 2006, **20**, 3681–92.

View Article Online
DOI: 10.1039/C6MT00045B

33 H. Yoon, J. P. Dehart, J. M. Murphy and S.-T. S. Lim, *J. Histochem. Cytochem.*, 2015, **63**, 114–28.

34 Y.-L. Tai, L.-C. Chen and T.-L. Shen, *Biomed Res. Int.*, 2015, **2015**, 690690.

35 N. A. Chatzizacharias, G. P. Kouraklis and S. E. Theocharis, *Histol. Histopathol.*, 2008, **23**, 629–50.

36 W. Liu, D. A. Bloom, W. G. Cance, E. V Kurenova, V. M. Golubovskaya and S. N. Hochwald, *Carcinogenesis*, 2008, **29**, 1096–107.

37 M. Z. Mehdi, G. Vardatsikos, S. K. Pandey and A. K. Srivastava, *Biochemistry*, 2006, **45**, 11605–15.

38 L. A. Cary, J. F. Chang and J. L. Guan, *J. Cell Sci.*, 1996, **109 (Pt 7**, 1787–94.

39 V. M. Golubovskaya, C. Nyberg, M. Zheng, F. Kweh, A. Magis, D. Ostrov and W. G. Cance, *J. Med. Chem.*, 2008, **51**, 7405–16.

40 I. Tanjoni, C. Walsh, S. Uryu, A. Tomar, J.-O. Nam, A. Mielgo, S.-T. Lim, C. Liang, M. Koenig, C. Sun, N. Patel, C. Kwok, G. McMahon, D. G. Stupack and D. D. Schlaepfer, *Cancer Biol. Ther.*, 2010, **9**, 764–77.

41 J. K. Slack-Davis, K. H. Martin, R. W. Tilghman, M. Iwanicki, E. J. Ung, C. Autry, M. J. Luzzio, B. Cooper, J. C. Kath, W. G. Roberts and J. T. Parsons, *J. Biol. Chem.*, 2007, **282**, 14845–52.

42 M. Z. Mehdi and A. K. Srivastava, *Arch. Biochem. Biophys.*, 2005, **440**, 158–64.

43 M. S. Bhuiyan, N. Shioda and K. Fukunaga, *Expert Opin. Ther. Targets*, 2008, **12**, 1217–27.

View Article Online
DOI: 10.1039/C6MT00045B

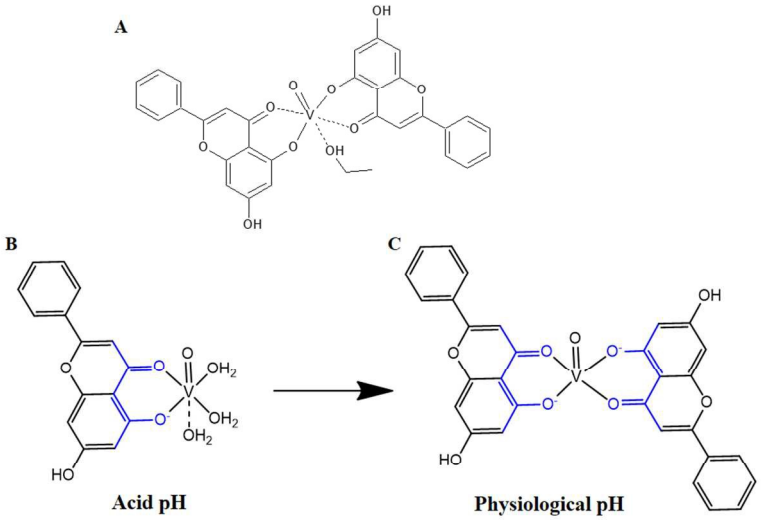

Figure 1
338x190mm (96 x 96 DPI)

View Article Online
DOI: 10.1039/C6MT00045B

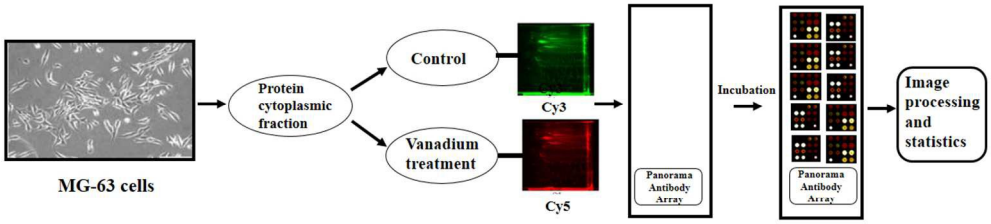

Figure 2
338x190mm (96 x 96 DPI)

View Article Online
DOI: 10.1039/C6MT00045B

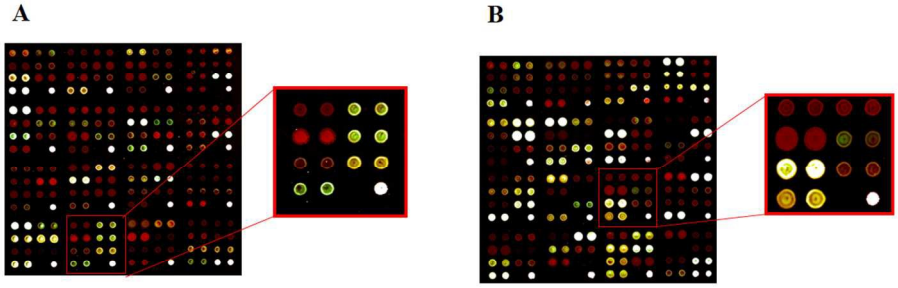

Figure 3
338x190mm (96 x 96 DPI)

View Article Online
DOI: 10.1039/C6MT00045B

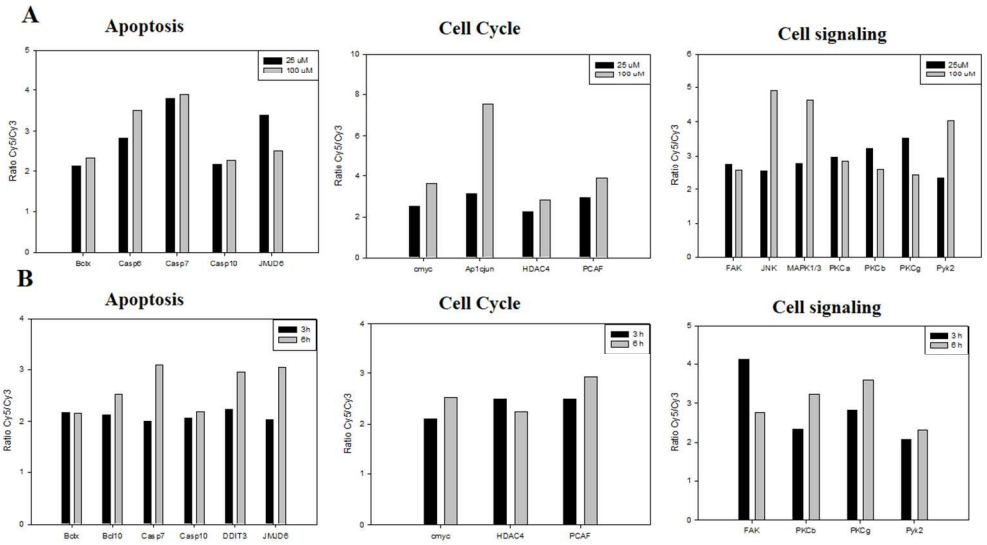

Figure 4
338x190mm (96 x 96 DPI)

View Article Online
DOI: 10.1039/C6MT00045B

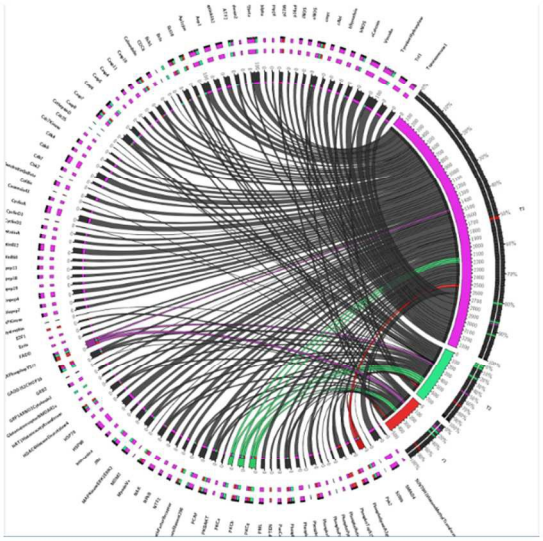

Figure 5
338x190mm (96 x 96 DPI)

View Article Online
DOI: 10.1039/C6MT00045B

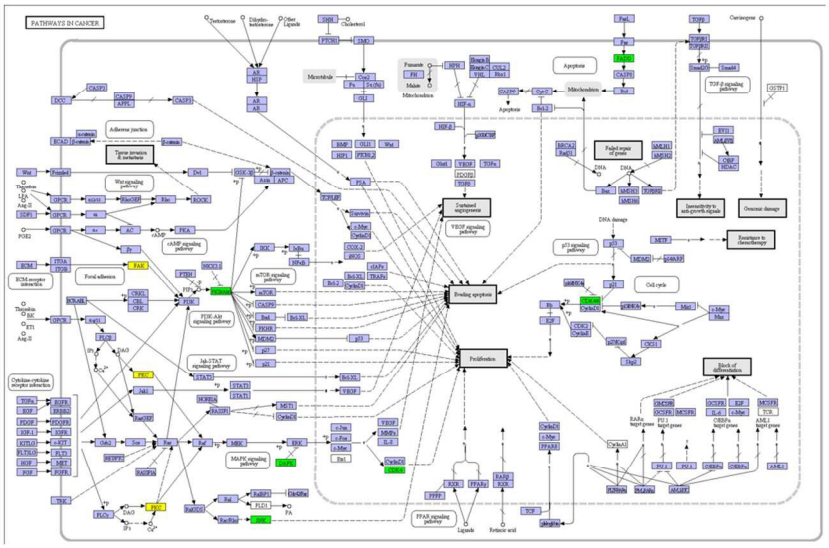

Figure 6A
338x190mm (96 x 96 DPI)

View Article Online
DOI: 10.1039/C6MT00045B

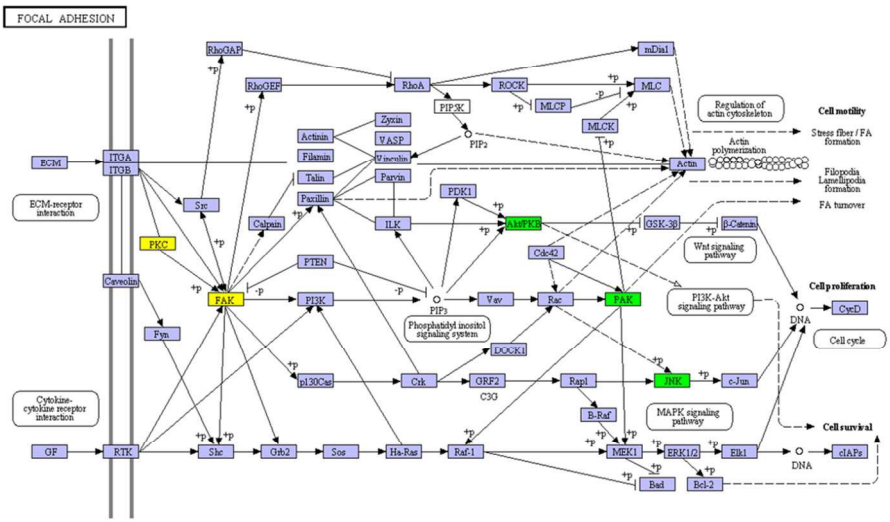

Figure 6B
338x190mm (96 x 96 DPI)